THREE-DIMENSIONAL BIOMEDICAL IMAGE DE-NOISING

V. Musoko * **and A. Procházka** *

* *Prague Institute of Chemical Technology*
Department of Computing and Control Engineering
Technická 1905, 166 28 Prague 6, Czech Republic
Phone: +420-224 354 198 Fax: +420-224 355 053
e-mail : Victor.Musoko@vscht.cz, A.Prochazka@ieee.org

Abstract: The paper presents the fundamental mathematical methods used in the analysis and processing of three-dimensional (3D) image objects. The methods to be discussed include 3D discrete Fourier transform (DFT) and Wavelet transform (WT). Firstly there is a need to generate an object for testing followed by its 3D visualization and the generation of the random noise. Computer visualization and processing is applied to the 3D biomedical image data.

Keywords: Discrete Fourier Transform, Three-Dimensional visualization, Wavelet Transform, Biomedical Image Analysis, Image De-Noising

1. INTRODUCTION

Several of today's imaging techniques (Bilgin and Marcellin 2000) produce three-dimensional (3D) data sets. Medical imaging techniques, such as computer tomography (CT) and magnetic resonance (MR), generate multiple slices in a single examination, with each slice representing a different cross section of the body part being imaged. However when transmitting these image volumes there is a possibility that noise is encountered during image transmission as pixel drop-outs. Noise elimination forms a fundamental problem in image processing.

The three-dimensional discrete Fourier transform is applied for noise rejection by the use of an appropriate window function in the frequency domain. Wavelet transform allows the image volume decomposition and reconstruction using selected threshold levels. The paper compares efficiency of the proposed methods. A series of de-noising and enhancement experiments is performed to verify the efficiency of the methods using 3D image volumes corrupted with random noise. The experimental results of the algorithms described are compared based on the quality of the de-noised image volumes. The algorithms are at first tested for the generated image objects and then applied to real magnetic resonance image (MRI) volumes for the biomedical 3D image applications.

The paper is organized as follows: Sections 4 and 5 present a brief overview of Fourier and wavelet transform techniques and their applications to multidimensional data. In Section 6 simulated and MR volumes are used to test de-noising performance of the proposed algorithms. The performance of the algorithms are investigated and compared using the mean square error (MSE) and signal-noise-ratio (SNR) criteria. Section 7 summarizes the paper and provides some of the possible solutions to improve the de-noising.

2. BIOMEDICAL IMAGE VISUALIZATION

Magnetic resonance imaging (MRI) is based on the absorption and emission of energy in the radio frequency range of the electromagnetic spectrum.

MRI produces an image of the nuclear magnetic resonance (NMR) signal in a thin slice through the human body for investigation of brain, liver, kidneys and other soft tissue organs. To form a 3D volume a continuous set of 2D data slices are stacked one on top of the other. Fig. 1 shows the original 20 frames of the MR brain image. A rendered 3D view of the stack of images is shown in Fig. 2. The three-dimensional array values are represented as $f[m, n, k]$ where $m = 1, \ldots, M$ represents the x-pixel co-ordinates, $n = 1, \ldots, N$ represents the y-pixel co-ordinates and $k = 1, \ldots, K$ are the corresponding slices.

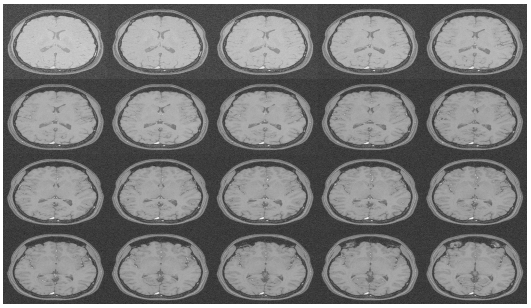

Fig. 1. Sequence of MR image slices

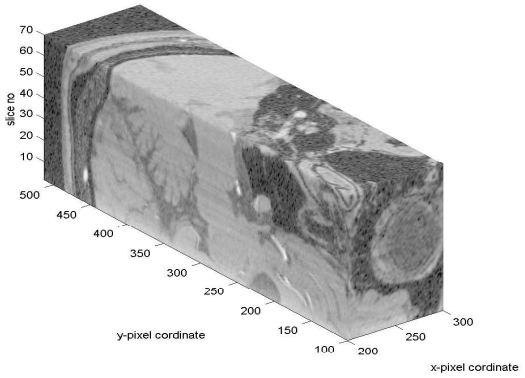

Fig. 2. The 3D model visualization

3. NOISE

When an image signal is received after transmission over some distance, it is oftenly corrupted with noise. The simplest model for the acquisition of noise by a signal is additive noise, which has the form

$$\tilde{f}(x) \;=\; \bar{f}(x) + \tilde{n}(x)$$

where $\tilde{f}(x)$...corrupted signal, $\bar{f}(x)$...original signal and $\tilde{n}(x)$ ...additive noise

Noise may be completely random and often noise is additive, simply causing the resulting signal/image to be sample by sample higher or lower than it should be. Random noise can also occur in short sections of the signal. This is called localized random noise and can be caused by abrupt disruptions in the transmission of the signal. In recent years, wavelets have been used to effectively minimize such type of noise.

4. DISCRETE FOURIER TRANSFORM

Discrete Fourier transform represent an efficient tool for image decomposition, analysis and its reconstruction.

4.1 *Two-dimensional Discrete Fourier Transform*

Two-dimensional discrete Fourier transform is used for the processing of image slices. Basis functions are sinusoids with frequency u in one direction times sinusoids with frequency v in the other. For an $M \times N$ image $f[m, n]$, these basis functions can be replaced for computational purposes by complex exponentials $e^{i2\pi um/M}$ and $e^{i2\pi vn/N}$ to evaluate the discrete Fourier transform

$$F[u, v] = \sum_{m=0}^{M-1} \sum_{n=0}^{N-1} f[m, n] e^{-i2\pi(um/M + vn/N)} \quad (1)$$

and inverse transform

$$f[m, n] = \frac{1}{MN} \sum_{u=0}^{M-1} \sum_{v=0}^{N-1} F[u, v] e^{i2\pi(um+vn)} \quad (2)$$

The point $F[u, v]$ in the frequency domain corresponds to the basis function with frequency u and frequency v.

The 2D Fourier transform is *linearly separable* i.e. the Fourier transform of a two-dimensional image is the Fourier transform of the rows followed by the Fourier transform of the resulting columns (or vice versa) as shown below.

$$\begin{aligned} F[u, v] &= \sum_{m=0}^{M-1} \sum_{n=0}^{N-1} f[m, n] e^{-i2\pi(um/M + vn/N)} \\ &= \sum_{m=0}^{M-1} \sum_{n=0}^{N-1} f[m, n]\; e^{-i2\pi um/M} e^{-i2\pi vn/N} \\ &= \sum_{m=0}^{M-1} \left[\sum_{n=0}^{N-1} f[m, n] e^{-i2\pi um/M} \right] e^{-i2\pi vn/N} \end{aligned}$$

The fast Fourier transform (FFT) is an efficient algorithm to calculate the DFT. N and M are commonly powers of 2 (for the FFT).

4.2 *Three-dimensional Discrete Fourier Transform*

Three-dimensional discrete Fourier transform of three-dimensional data values $f[m, n, k]$, where

$m = 0, 1 \ldots M-1$, $n = 0, 1 \ldots N-1$ and $k = 0, 1 \ldots K-1$ is here defined by the relation

$$F[u,v,w] = \sum_{m=0}^{M-1} \sum_{n=0}^{N-1} \sum_{k=0}^{K-1} f[m,n,k] e^{-i2\pi(\frac{um}{M} + \frac{vn}{N} + \frac{wk}{K})} \tag{3}$$

The inverse Fourier transform is

$$f[m,n,k] = C \sum_{u=0}^{M-1} \sum_{v=0}^{N-1} \sum_{w=0}^{K-1} F[u,v,w] e^{i2\pi(\frac{um}{M} + \frac{vn}{N} + \frac{wk}{K})} \tag{4}$$

for $u = 0, 1 \ldots M-1$, $v = 0, 1 \ldots N-1$, $w = 0, 1 \ldots K-1$ and $C = \frac{1}{MNK}$

5. DISCRETE WAVELET TRANSFORM

Discrete Wavelet transform (DWT) (Newland 1994) decomposes a signal into a two-dimensional function of time and scale. Wavelet analysis is a modification of Fourier analysis, where functions other than sine and cosine are used as the basis functions which enable localization in space and frequency. Wavelet functions used for signal analysis are derived from the initial function forming basis for the set of basis functions.

Two types of basis functions normally used are

- Scaling function $\Phi_{mk}(t)$

$$\Phi_{mk}(t) = 2^{-\frac{m}{2}} \Phi_0(2^{-m}t - k) \tag{5}$$

- Wavelet $\Psi_{mk}(t)$

$$\Psi_{mk}(t) = 2^{-\frac{m}{2}} \Psi_0(2^{-m}t - k) \tag{6}$$

where m stands for dilation or compression and k is the translation index. Every basis function Ψ is orthogonal to every basis function Φ.

In this paper we are going to use the Haar wavelet which is the simplest of all the wavelets. One nice feature of the Haar wavelet transform is that the transform is equal to its inverse. The Haar mother wavelet (Fig. 3) is defined as follows:

$$\Phi_0(t) = \begin{cases} 1 & 0 \le t \le 1 \\ 0 & \text{otherwise} \end{cases}$$

$$\Psi_0(x) = \begin{cases} 1 & 0 \le t \le \frac{1}{2} \\ -1 & \frac{1}{2} \le t \le 1 \\ 0 & \text{otherwise} \end{cases}$$

The wavelet transform (Khalil and Shaheen 1999) is implemented using a pair of filters: a low-pass filter L and a high-pass filter H, which split a signal's bandwidth in two halves.

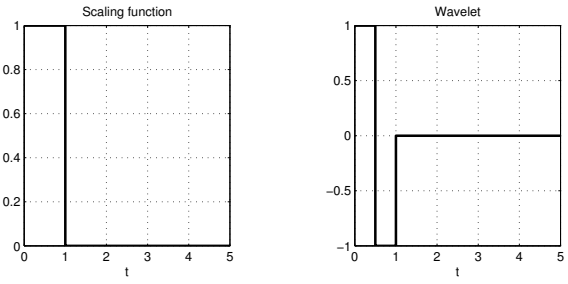

Fig. 3. Scaling function and Haar wavelet

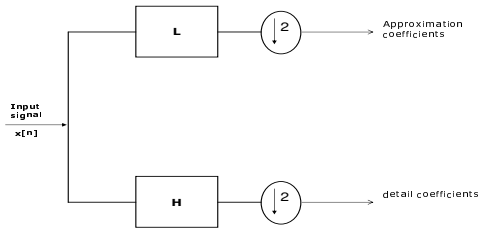

Fig. 4. Signal decomposition

The 1D forward wavelet transform of a discrete-time signal $x[n]$ $(0 \le n < N)$ is performed by convolving that signal with both a half-band low-pass filter L and high-pass filter H and down-sampling by two.

$$c[n] = \sum_{k=0}^{P-1} s[k]\, x[n-k] \qquad d[n] = \sum_{k=0}^{P-1} w[k]\, x[n-k] \tag{7}$$

where $c[n]$ represent the approximation coefficients for $n = 0, 1, 2 \ldots, P-1$ $(P = \frac{N}{2})$, $d[n]$ are the detail coefficients, s and w respectively, are coefficients of the discrete-time filters L and H

$$\{s[k]\}_{n=0}^{P-1} = (s[0], s[1], \ldots, s[P-1])$$
$$\{w[k]\}_{n=0}^{P-1} = (w[0], w[1], \ldots, w[P-1])$$

5.1 *Three-dimensional Wavelet Transform*

Discrete Wavelet Transform (DWT) (Pinnamaneni and Meyer 2001) is a separable, sub-band transform. Although nonseparable wavelets can also be used for multidimensional signals, such filters are much harder to design than are separable filters. As a result, their use has been limited in image processing applications. 3D wavelets can be constructed as separable products of 1D wavelets by successively applying a 1D analyzing wavelet in three spatial directions (x,y,z).

Fig. 5 shows a separable 3D decomposition of a volume. The volume $F(x,y,z)$ (Khalil and Shaheen 1999) is firstly filtered along the x dimension, resulting in a low-pass image $L(x,y,z)$ and a high-pass image $H(x,y,z)$. Since the size of L and H along the x dimension is now half that of

$F(x, y, z)$, down-sampling of the filtered volume in the x dimension by two can be done without loss of information. The down-sampling is done by dropping each odd filtered value. Both L and H are then filtered along the y dimension, resulting in four decomposed sub-volumes: LL, LH, HL and HH. Once again, we can down-sample the sub-volumes by two, this time along the z dimension. Then each of these four sub-volumes are then filtered along the z dimension, resulting in eight sub-volumes: *LLL, LLH, LHL, LHH, HLL, HLH, HHL* and *HHH* (see Fig 5).

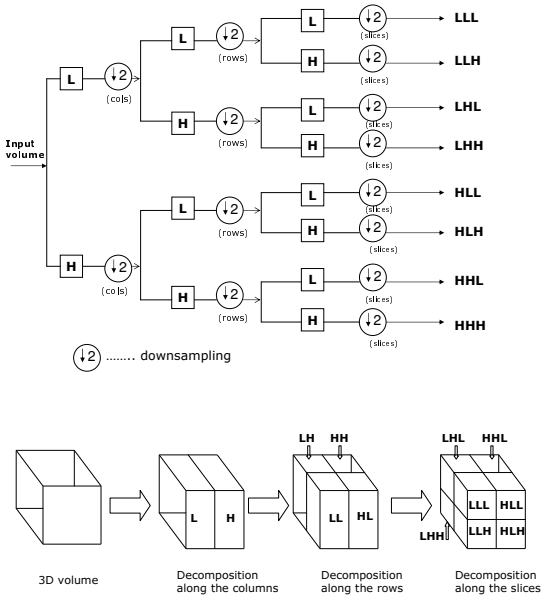

Fig. 5. Three-dimensional WT decomposition

5.2 *Wavelet thresholding - de-noising*

After decomposition it is possible to modify resulting coefficients before the reconstruction to eliminate undesirable signal components. To implement wavelet thresholding the so called wavelet shrinkage algorithm is applied which consists of the following steps:

- Perform the forward wavelet transform
- Estimate a threshold
- Choose shrinkage rule and apply the threshold according to this rule
- Perform the inverse transform using the thresholded coefficients

In our experiments we used the universal threshold, soft shrinkage rule and scaled MAD (median absolute deviation) noise estimator.

The universal threshold is given by:

$$\lambda \;=\; \sigma\sqrt{2\log(N)}$$

where N is the size of the coefficient arrays.

Level dependent threshold

$$\lambda_k \;=\; \sigma_k\sqrt{2\log(N)}$$

where the scaled MAD noise estimator is computed by:

$$\sigma_k = \frac{MAD_k}{0.6745} = \frac{(median(|\omega_i|))_k}{0.6745}$$

ω_i are the coefficients for a given sub-band k

The threshold estimation method is repeated for each sub-band separately, because the sub-bands exhibit significantly different characteristics.

Estimation of the noise variance σ_k is done by using the robust median estimator in the highest sub-band of the wavelet transform

The shrinkage rule define how we apply the threshold. There are two main approaches.

Hard thresholding (Fig 6b) deletes all coefficients that are smaller than the threshold λ and keeps the others unchanged. The hard thresholding is defined as follows:

$$\bar{c}_s(k) = \begin{cases} \text{sign } c(k)\ (|\,c(k)\,|) & \text{if } |\,c(k)\,| > \lambda \\ 0 & \text{if } |\,c(k)\,| \leq \lambda \end{cases} \qquad (8)$$

where λ is the threshold and the coefficients that are above the threshold are the only ones to be considered.

Soft thresholding (Fig 6c) deletes the coefficients under the threshold, but scales the ones that are left. The general soft shrinkage rule is defined by:

$$\bar{c}_s(k) = \begin{cases} \text{sign } c(k)\ (|\,c(k)\,| - \lambda) & \text{if } |\,c(k)\,| > \lambda \\ 0 & \text{if } |\,c(k)\,| \leq \lambda \end{cases} \qquad (9)$$

For an illustration of what has been described above a linear signal is thresholded according to the methods described using a thresold of 0.5 (Fig. 6).

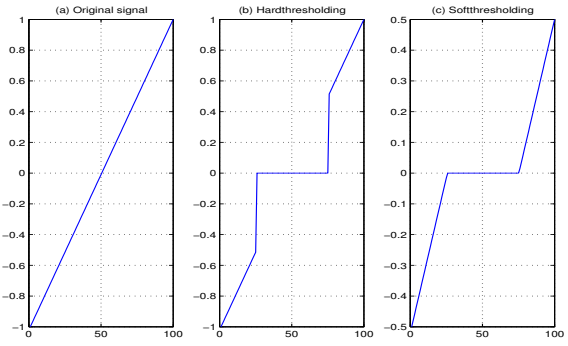

Fig. 6. An example of soft-thresholding and hard-thresholding to an original signal using a threshold $\lambda = 0.5$

5.3 *Reconstruction*

After modifying the coefficients we can apply the inverse transform by convolving with the respective low-pass and high-pass synthesis filters as described in various books ((Strang and Nguyen 1996), (Vetterli 1992)). The resulting structure is presented in Fig. 7.

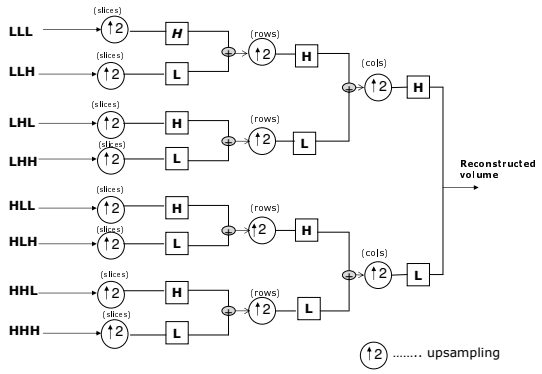

Fig. 7. Three-dimensional WT reconstruction

6. RESULTS

The algorithms were applied to simulated volume and MRI sub-volume. Both volumes are corrupted with randomly distributed noise generated using the MATLAB `rand` function.

These methods are compared using the mean square error (MSE), signal-noise-ratio (SNR) and visual criteria. Assuming that the original uncorrupted volume is known our goal is to remove the noise, or 'de-noise' and to obtain an estimate of $\tilde{f}[m,n,k]$ of $f[m,n,k]$ which gives a reasonable small value of the mean square error (MSE). The MSE is computed relative to the original image volume i.e. it measures the difference between the values of the corresponding pixels from the two volumes.

MSE is calculated using the following equation:

$$MSE = C \sum_{m=0}^{M-1} \sum_{n=0}^{N-1} \sum_{k=0}^{K-1} \Big(f[m,n,k] - \tilde{f}[m,n,k] \Big)^2 \tag{10}$$

where $C = \frac{1}{MNK}$, $f[m,n,k]$ and $\tilde{f}[m,n,k]$ represent the original volume and the filtered or 'de-noised' volume respectively.

6.1 *Results from simulated realistic data*

The simulated volume consists of a number of $64 \times 64 \times 8$ three-dimensional data.

The 3D Haar wavelet transform has been used to de-noise the noisy volume. Fig. 9 shows a plot of

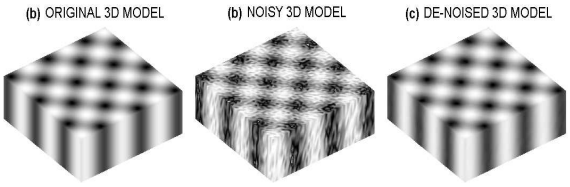

Fig. 8. Application of Fourier transform to a noisy simulated image volume

the coefficients of a one level of the Haar transform. The horizontal lines shown in the graph are the soft thresholding levels of 0.5. The effect of this thresholding will set all the values in the filtered signal that have an absolute value less than 0.5 to zero. Applying the given threshold level and taking the inverse of the result a de-noised volume is obtained as shown in Fig 9c.

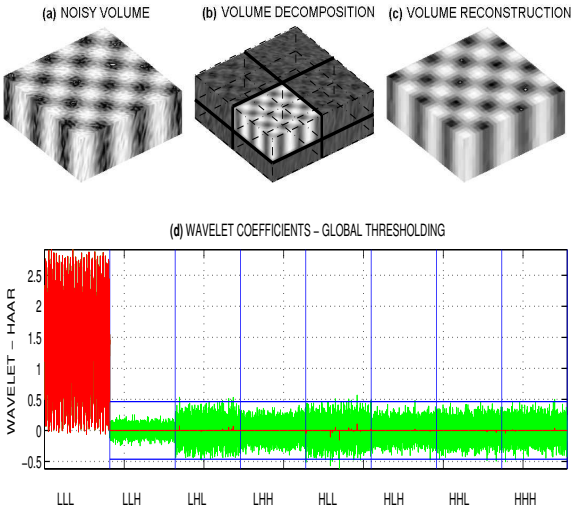

Fig. 9. The 3D decomposition and reconstruction

Table 1. QUALITATIVE ANALYSIS - SIMULATED MODEL

Type of method	*MSE*
Noisy image	0.01488
DFT	0.000005
Global thresholding	0.003480
Level-dependent	0.003487

6.2 *Results from real MRI data*

Fig. 10 shows the de-noised MR sub-volume after the application of Fourier transform.

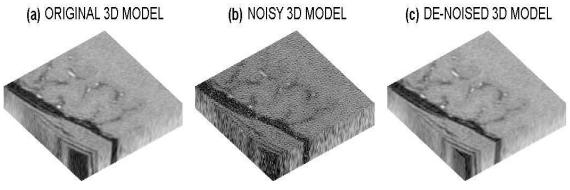

Fig. 10. The 3D visualization for the reconstructed MRI volume

We applied 3-D Haar wavelet transform algorithm to an MRI scan of a human brain (128 x 128 x 16). The figure which follows (Fig. 11) shows a one level decomposition of the 3D volume.

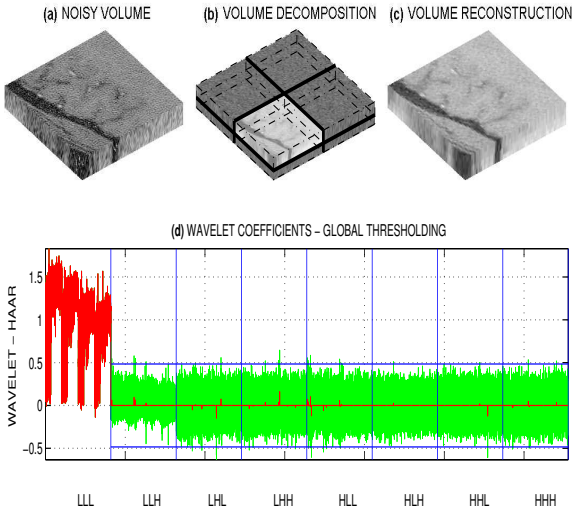

Fig. 11. The 3D decomposition and reconstruction of MR image volume

The MSE (mean squared error) information obtained from the proposed algorithms is included in Table 2. The visual quality of the results can be seen from Fig. 11.

Table 2. QUALITATIVE ANALYSIS - MRI VOLUME

Type of method	*MSE*	*SNR*[dB]
Noisy image	0.014580	13.7537
DFT	0.000070	26.8482
Global thresholding	0.002618	19.3300
Level-dependent	0.002620	18.6147

7. CONCLUSIONS

In this paper we presented the generalization of the DWT to 3D case. The resulting algorithm has been used for the processing of noisy MR image volumes. Fourier transform has been just used as a method of verification as we have used an ideal filter window function which completely eliminated the noise. Future work will involve the use other types of wavelets like the Daubechies which possible might give better results than the ordinary and simple Haar wavelet.

ACKNOWLEDGMENTS

The work has been supported by the research grant of the Faculty of Chemical Engineering of the Institute of Chemical Technology, Prague No. MSM 223400007. This support is gratefully acknowledged.

8. REFERENCES

Bilgin, A. and M.W. Marcellin (2000). Three dimensional image compression with integer wavelet transforms. *Applied Optics*.

Burrus, C. S., R.A. Gopinath and H. Guo (1998). *Introduction to Wavelets and Wavelet Transforms*. Prentice Hall. New Jersey.

Donoho, D.L. (1995). De-noising by soft thresholding. *IEEE Trans. on Information Theory* **38(2)**, 613–627.

Donoho, D.L. and I.M. Johnstone (1994). Ideal spatial adaption via wavelet shrinkage. *Biometrika* **81(3)**, 425–455.

Kamath, C. and I.K. Fodor (2002). Undecimated wavelet transforms for image de-noising. *Applied Scientific Computing, Lawrence Livermore National Laboratory*.

Khalil, H. and S. Shaheen (1999). Three dimensional video compression. *IEEE Transactions on Image Processing* **8**, 762–773.

Newland, D. E. (1994). *An Introduction to Random Vibrations, Spectral and Wavelet Analysis*. third ed.. Longman Scientific & Technical. Essex, U.K.

Pinnamaneni, P. and J. Meyer (2001). Three-dimensional wavelet compression. *2nd Annual Tri-State Engineering Society Meeting*.

Strang, G. and T. Nguyen (1996). *Wavelets and Filter Banks*. Wellesley-Cambridge Press.

Vetterli, M. (1992). Wavelets and filter banks theory and design. *IEEE Trans. Signal Processing* **40**(9), 2207–2232.